Implementation And Tuning a Model Predictive Control Scheme for a Single Ended Primary Inductor Converter

2025 9th International Symposium on Electrical and Electronics Engineering (ISEEE) | 979-8-3315-7666-0/25/$31.00 ©2025 IEEE | DOI: 10.1109/ISEEE67817.2025.11304836

Andronic Michel RAJAONA
Energy Systems Engineering
Karadeniz Technical University
Trabzon, Türkiye
michel47rajaona@gmail.com
ORCID: 0000-0001-5570-9154

Ömür AKYAZI
Energy Systems Engineering
Karadeniz Technical University
Trabzon, Türkiye
oakyazi@ktu.edu.tr
ORCID: 0000-0001-6266-2323

Yahya DANAYİYEN
Electrical and Electronics Engineering
Karadeniz Technical University
Trabzon, Türkiye
yahya@ktu.edu.tr
ORCID: 0000-0002-8679-4088

***Abstract*— In this paper, an optimized Model Predictive Control (MPC) strategy is proposed for the Single-Ended Primary-Inductor Converter (SEPIC) operating under parameter and load variations. The controller is designed using a discrete-time state-space model to regulate the output voltage V_o, input voltage V_{in}, and load resistance R_{load} while satisfying duty-cycle constraints. Initially, random values of the control horizon N_c, prediction horizon N_p, output error weight Q, and control effort weight R_{mpc} were applied. The system performance was then analyzed using the Integral of Time-weighted Absolute Error (ITAE) criterion, represented through a 3D surface plot of ITAE versus Q and R_{mpc}. This analysis enabled the identification of optimal parameters that improved system stability and dynamic performance. The optimized MPC was subsequently tested under variations in input voltage, output reference, and load resistance, maintaining accurate tracking, fast settling, and minimal overshoot. The results confirm that the proposed ITAE-driven MPC effectively enhances SEPIC converter performance under dynamically changing conditions.**

Keywords*— *Sepic Converter, Optimization, Model Predictive Control, ITAE

I. INTRODUCTION

SEPIC converter is known for its ability to both step up and step down the input voltage without inverting polarity and can be considered as a buck-boost converter. This ability makes it a good choice in applications where the input voltage may fluctuate around the reference output level, such as battery-powered systems, renewable energy systems, or even automotive electronics. However, due to its inherent nonlinearity and fast-switching dynamics, designing a controller that ensures precise output voltage regulation while respecting operational constraints is a significant challenge [1]-[5].

Conventional linear controllers [6]-[11] such as proportional integral (PI) regulators are simple and easy to implement but may lead to poor transient performance and overshoot when the converter operates over a wide range of operating points . Advanced nonlinear or adaptive techniques improve robustness but usually require complex parameter tuning and high computational cost. Therefore, a control approach capable of handling system constraints and nonlinearities in a systematic way is highly desirable [12]. MPC is a powerful strategy to manage such systems, with a strong ability to handle multi-variable dynamics, constraints and future setpoint changes in a systematic and optimal manner. MPC predicts the future behavior of the system over specified horizon using a mathematical model and determines the optimal control action by minimizing a cost function [13], [14]. Abdel-Rahim et al. [15] proposed an MPC-based MPPT algorithm for a modified SEPIC converter that effectively reduces the number of sensors while maintaining high efficiency under varying irradiance. However, the parameter identification process and model coefficients were treated as fixed, limiting controller robustness when converter parasitics or temperature-dependent variations occur. Similarly, Kandasamy et al. [16] combined interleaved SEPIC topology with MPC for electric-vehicle charging, yet their design relied on nominal component values and heuristic tuning of the predictive model, leading to performance degradation under wide input-voltage changes.

Unlike previous studies that selected MPC weighting matrices heuristically, this work introduces a systematic tuning method based on the Integral of Time-weighted Absolute Error (ITAE) criterion. The ITAE function captures both transient and steady-state behavior, enabling automatic and balanced tuning of the predictive control weights. The proposed ITAE-driven MPC thus ensures faster response, improved voltage regulation, and higher robustness against parameter variations in the SEPIC converter, using a discrete-time linearized state-space model.

II. PRINCIPLE OF OPERATION

The Single-Ended Primary-Inductor Converter (SEPIC), shown in Fig. 1, is a non-inverting DC–DC topology capable of stepping the output voltage above or below the input level. It consists of two inductors, two capacitors, a diode, and a single switch that transfer energy through controlled charge–discharge cycles. Operating in continuous conduction mode (CCM) ensures smooth current flow and low ripple, resulting in efficient and stable voltage regulation over wide input variations. To illustrate its behavior, the converter's operation is analyzed over a full switching cycle in two intervals: ON-state and OFF-state of the main switch.

A. ON state

When the switch Q_1 is turned on, both inductors (L_1 and L_2) store energy from the input source v_i. The diode D_1 becomes reverse-biased, isolating the output stage, while the

979-8-3315-7666-0/25/$31.00 ©2025 IEEE.

Authorized licensed use limited to: ULAKBIM UASL - KARADENIZ TECHNICAL UNIVERSITY. Downloaded on December 31,2025 at 11:57:25 UTC from IEEE Xplore. Restrictions apply.

coupling capacitor C_1 transfers energy between the inductors. During this interval, the inductor currents (i_{L_1}, i_{L_2}) increase linearly, and the output capacitor C_2 supplies the load, maintaining voltage continuity. The energy stored in the magnetic components during this state determines the converter's dynamic and steady-state performance.

B. OFF State

When the switch is turned off, the diode D_1 becomes forward-biased, providing a current path for the load. The energy stored in the first inductor (L_1) is transferred to the second inductor (L_2) through the coupling capacitor (C_1), while L_2 simultaneously delivers energy to the output via the diode. Both inductor currents decrease linearly, ensuring continuous conduction and maintaining the output voltage v_o through the combined discharge of the inductors and capacitors.

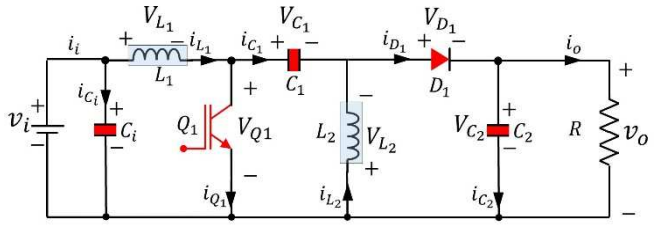


Fig. 1. Circuit diagram of a SEPIC converter

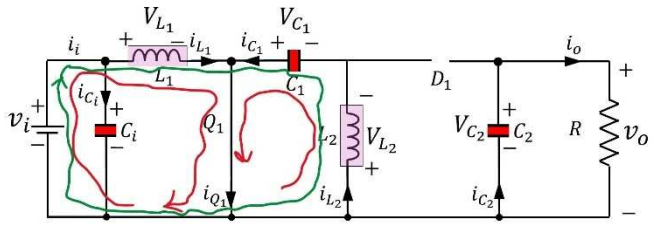


Fig. 2. ON state

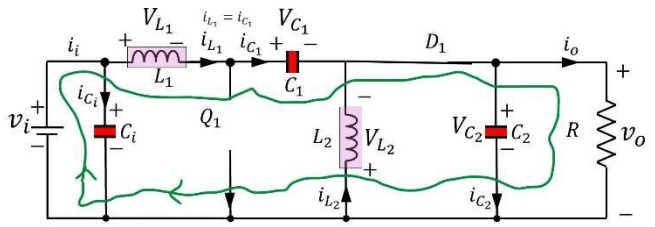


Fig. 3. OFF state

C. State-Space Model For Controller Design

To design a predictive controller capable of ensuring fast and accurate voltage regulation, an accurate mathematical model of the SEPIC converter is required. In this section, the converter is modeled in the state-space form based on the averaged circuit equations derived for both ON and OFF states. The resulting discrete-time model is then employed in the formulation of the Model Predictive Control (MPC) algorithm, where the control input (duty ratio) is optimized by minimizing a cost function defined in terms of the predicted output voltage error and control effort. The dynamic behavior of the converter model is described by the following four state variables, which form the state vector $x(t)$ given in (1).

$$x(t) = [i_{L_1}(t) \quad V_{C_1}(t) \quad i_{L_2}(t) \quad v_0(t)]^T \tag{1}$$

The control input for this model is the switch duty cycle, denoted as $u(t)$. The behavior of the system is defined by the following set of linear differential equations. This model treats the duty cycle $u(t)$ as a direct, continuous scaling factor for the input voltage's effect on the first inductor's current.

$$\frac{di_{L1}}{dt} = -\frac{1}{L_1} i_{L1} + \frac{V_{in}}{L_1} u(t) \tag{2}$$

$$\frac{dv_{C1}}{dt} = \frac{1}{C_1} i_{L1} - \frac{1}{R.C_1} v_{C1} - \frac{1}{C_1} i_{L2} \tag{3}$$

$$\frac{di_{L2}}{dt} = \frac{1}{L_2} v_{C1} - \frac{1}{L_2} i_{L2} \tag{4}$$

$$\frac{dv_o}{dt} = \frac{1}{C_2} i_{L2} - \frac{1}{R.C_2} v_o \tag{5}$$

The above differential equations can be expressed in the standard continuous-time state-space form:

$$\dot{x}(t) = Ax(t) + Bu(t) \tag{6}$$

Where:

$$A = \begin{bmatrix} -\frac{1}{L_1} & 0 & 0 & 0 \\ \frac{1}{C_1} & -\frac{1}{R.C_1} & -\frac{1}{C_1} & 0 \\ 0 & \frac{1}{L_2} & -\frac{1}{L_2} & 0 \\ 0 & 0 & \frac{1}{C_2} & -\frac{1}{R.C_2} \end{bmatrix}, \quad B = \begin{bmatrix} \frac{V_{in}}{L_1} \\ 0 \\ 0 \\ 0 \end{bmatrix}.$$

The output of the system is defined as the voltage v_o across the output capacitor C_2. Thus, the output equation is expressed as:

$$y(t) = Cx(t) + Du(t) \tag{7}$$

Where $C = [0 \quad 0 \quad 0 \quad 1]$, $D = [0]$.

This complete continuous-time Linear Time-Invariant (LTI) model serves as the foundation for the predictive control design presented in the next section.

III. Model Predictive Control

Model Predictive Control (MPC) enhances converter performance through its ability to predict future system behavior and adjust the control input in real time to minimize the deviation from the reference value. To implement the MPC algorithm digitally, the continuous-time SEPIC model is discretized using a sampling period T_s. The discrete system matrices are obtained from the continuous model as

$$A_d = e^{ATs}, \quad B_d = \left(\int_0^{Ts} e^{A\tau} d\tau\right) B \tag{8}$$

Authorized licensed use limited to: ULAKBIM UASL - KARADENIZ TECHNICAL UNIVERSITY. Downloaded on December 31,2025 at 11:57:25 UTC from IEEE Xplore. Restrictions apply.

Where $T_s = \frac{1}{nf_{sw}}$, is determined by the converter switching frequency f_{sw} and the sampling ratio n. The resulting discrete-time model is expressed as:

$$x_{k+1} = A_d x_k + B_d u_k,\ y_k = C_d x_k \tag{9}$$

where x_k is the state vector at time step k, and the discrete matrices A_d, B_d, and C_d are computed from the continuous matrices A, B and C. This discrete model is used for all future predictions.

A. Output prediction model

The core of MPC is its ability to predict future outputs over a prediction horizon of N_p steps. The predicted output sequence can be expressed in a compact matrix form. The vector of future control inputs over a control horizon N_c is denoted as:

$$U_k = \begin{bmatrix} u_k \\ u_{k+1} \\ \vdots \\ u_{k+N_c-1} \end{bmatrix} \tag{10}$$

The vector of predicted future outputs over the prediction horizon N_p is denoted as:

$$Y_k = \begin{bmatrix} y_{k+1} \\ y_{k+2} \\ \vdots \\ y_{k+N_p} \end{bmatrix} \tag{11}$$

The relationship between the current state x_k, future controls U_k, and future outputs Y_k is given in (12)

$$Y_k = \Phi x_k + \Gamma U_k \tag{12}$$

Where:

$$\Phi = \begin{bmatrix} C_d A_d \\ C_d A_d^2 \\ \vdots \\ C_d A_d^{N_p} \end{bmatrix},\ \Gamma = \begin{bmatrix} C_d B_d & 0 & \cdots & 0 \\ C_d A_d B_d & C_d B_d & \cdots & 0 \\ \vdots & \ddots & \ddots & \vdots \\ C_d A_d^{N_p-1} B_d & C_d A_d^{N_p-2} B_d & \cdots & C_d A_d^{N_p-N_c} B_d \end{bmatrix}.$$

The matrices Φ and Γ are constructed from the discrete system matrices A_d, B_d and C_d.

B. Cost function formulation

The optimal control sequence is found by minimizing a quadratic cost function J which is defined in (13) at each time step k. The cost function penalizes the squared error between the predicted output (y_{k+i}) and the reference (r_{k+i}), as well as the magnitude of the control inputs (u_{k+j}).

$$J = \sum_{i=1}^{N_p} (y_{k+i} - r_{k+i})^2 Q + \sum_{j=0}^{N_c-1} (u_{k+j})^2 R \tag{13}$$

Where r is the reference vector. In matrix form, (13) can be written as follows:

$$J = (Y_k - V_{ref})^T Q (Y_k - V_{ref}) + U_k^T R_{mpc} U_k \tag{14}$$

where, Q and R_{mpc} are weighting matrices that tune the controller's performance. Substituting the prediction equation into the cost function yields:

$$J = (\Phi x_k + \Gamma U_k - V_{ref})^T Q (\Phi x_k + \Gamma U_k - V_{ref}) + U_k^T R_{mpc} U_k \tag{15}$$

Expanding (15) and grouping terms with respect to the decision variable U_k transforms the cost function into a standard quadratic form suitable for optimization solvers as follows:

$$\min_{U_k} \frac{1}{2} U_k^T \mathrm{H} U_k + f^T U_k \tag{16}$$

where the Hessian matrix H and the linear term vector f are defined as in (17) and (18).

$$H = 2(\Gamma^T Q \Gamma + R_{mpc}) \tag{17}$$

$$f = 2\Gamma^T Q (\Phi x_k - V_{ref}) \tag{18}$$

C. Integral of Time-weighted Absolute Error (ITAE) in discrete-time

The Integral of Time-weighted Absolute Error (ITAE) is a widely used performance index that evaluates both transient and steady-state characteristics of a control system. Unlike conventional error metrics that treat all deviations equally, the ITAE criterion penalizes errors occurring at later time steps more heavily, thereby promoting fast settling and minimally sustained oscillations. Since the SEPIC converter is modeled and controlled in discrete time with a sampling period T_s, the discrete-time ITAE can be expressed as:

$$ITAE = Ts. \sum_{k=1}^{N} k\ .|V_{ref} - V_o[k]| \tag{19}$$

where V_{ref} is the reference output voltage, $V_o[k]$ is the actual output voltage at sample k, and N is the total number of samples considered within the evaluation window.

A smaller ITAE value corresponds to faster response, reduced overshoot, and minimal steady-state error, indicating superior tracking performance. Conversely, a higher ITAE value reflects sluggish dynamics or oscillatory behavior. In this work, the ITAE criterion is incorporated into the MPC cost function to systematically determine the optimal weighting matrices (Q and R_{mpc}), ensuring a balanced trade-off between transient speed and steady-state precision.

D. Closed-loop iteration

At each time step, the MPC loop measures the current state, x_k, to construct the prediction model using matrices Φ and Γ. The cost function and constraints are then formulated into a Quadratic Program (QP), which is solved to find the optimal control sequence, U_k^*.Following the receding horizon strategy, only the first control input of this sequence is applied. Finally, the system updates to a new state, and the entire process repeats. Fig. 4 shows the close loop system. This results in a closed-loop predictive controller that adjusts the duty cycle in real-time to maintain the output voltage at its reference value.

Authorized licensed use limited to: ULAKBIM UASL - KARADENIZ TECHNICAL UNIVERSITY. Downloaded on December 31,2025 at 11:57:25 UTC from IEEE Xplore. Restrictions apply.

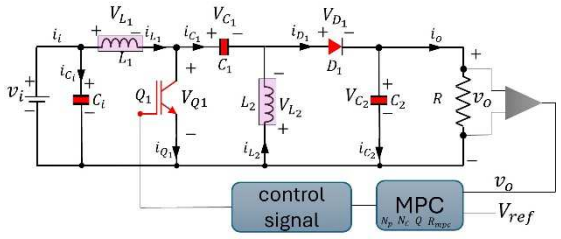


Fig. 4. Closed-loop SEPIC with MPC

IV. Implementation

The proposed ITAE-based MPC control strategy was modeled and tested in the MATLAB/Simulink environment using the discrete-time state-space representation of the SEPIC converter. To evaluate the controller's adaptability and robustness, three simulation scenarios were defined: **constant-parameter**, **random-parameter**, and **optimized-parameter** cases. Each scenario reflects a different operating condition to analyze how parameter variations affect dynamic response and steady-state accuracy.

A. Application under constant values

The constant-parameter scenario was simulated using the nominal SEPIC converter values listed in Table I (from [1]), representing a 200 W system with a 24 V input, 48 V output, and 50 kHz switching frequency. The converter was modeled in MATLAB/Simulink, including full converter dynamics and MPC control structure. The initial MPC parameters in Table II were used to assess baseline performance. Figs. 5–7 present the system response, showing output voltage tracking, duty cycle variation, and absolute error under nominal operating conditions.

TABLE I. PARAMETERS OF THE SYSTEM

Parameters	Values
Input voltage (V_{in})	24V
Output voltage (V_0)	48V
Power (P)	200W
Switching frequency (fsw)	50kHz
Sampling time (Ts)	2µs
Inductor (L_1)	38µH
Inductor (L_2)	38µH
Capacitor (C_1)	1µF
Capacitor (C_2)	120µF

TABLE II. RANDOM MPC PARAMETERS

Parameters	Values
Control horizon (N_c)	5
Predictive horizon (N_p)	80
Weight on output error (Q)	2000
Weight on control effort (R_{mpc})	80

Fig. 5 shows that the output voltage rapidly reaches the 48 V reference with a slight overshoot around 1ms before stabilizing just below the target. The duty cycle exhibits strong corrective action, and the absolute error converges to zero within 0.15ms, indicating fast dynamic response. The minor oscillations are due to non-optimized MPC parameters. Fig. 6–7 present the internal state trajectories, signed error, and predicted output voltage. The inductor current i_{L1} settles smoothly, while v_{C1} and i_{L2} remain nearly constant. The output voltage V_o closely follows the reference, and the signed error quickly converges to zero. The MPC prediction at 2 ms confirms anticipatory stabilization with slight under-tracking. As shown in Fig. 7, the system demonstrates good dynamics but slight instability, reflected by an ITAE of 0.92. By minimizing the ITAE surface, optimized parameters $Q = 1$ and $R_{mpc} = 100$ were obtained, reducing ITAE to 0.53 while keeping N_c and N_p unchanged. The updated MPC parameters in Table III are then applied in the second simulation to assess performance improvement.

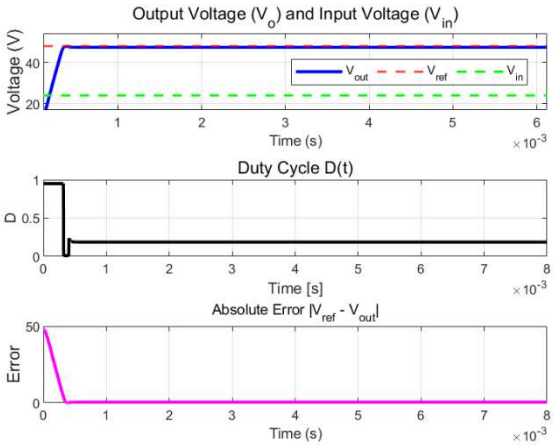


Fig. 5. Output voltage, duty cycle and absolute error in the first application

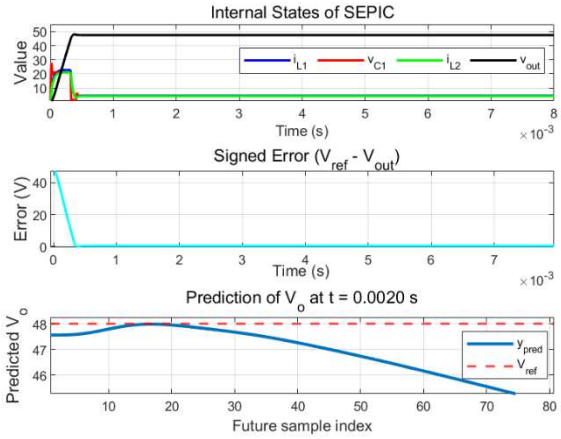


Fig. 6. Internal states of SEPIC signed error, prediction of output voltage in the first application

TABLE III OPTIMIZED MPC PARAMETERS

Parameters	Values
Control horizon (N_c)	5
Predictive horizon (N_p)	80
Weight on output error (Q)	1
Weight on control effort (R_{mpc})	100

Authorized licensed use limited to: ULAKBIM UASL - KARADENIZ TECHNICAL UNIVERSITY. Downloaded on December 31,2025 at 11:57:25 UTC from IEEE Xplore. Restrictions apply.

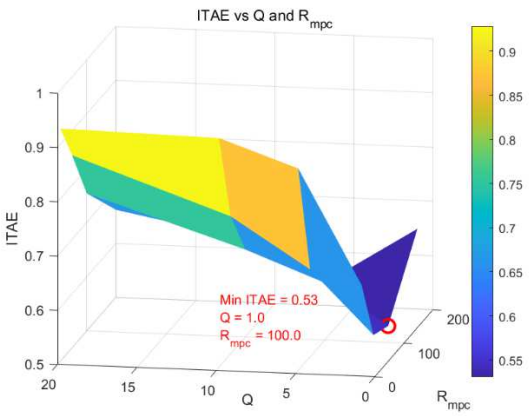


Fig. 7. *ITAE* vs Q and R_{mpc}

To validate the effectiveness of the optimization, the system was simulated a second time using the optimized MPC parameters listed in Table III. The corresponding results are presented in Figs. 8–10. Fig. 8 shows that the output voltage rapidly reaches the 48 V reference without overshoot. The duty cycle responds immediately and stabilizes, while the absolute error converges to nearly zero at around 1.2ms, indicating excellent steady-state stability. Fig. 9 illustrates the internal state responses of the SEPIC converter. The currents i_{L1} and i_{L2}, as well as the coupling capacitor voltage v_{C1}, exhibit fast transient dynamics and settle to steady-state conditions within approximately 2 ms. The signed error converges smoothly to zero with no observable oscillations, confirming improved controller performance. Fig. 10 presents the evolution of the duty cycle $D(t)$. The outer red dashed circle and inner green dashed circle denote the upper ($D_{max} = 0.95$) and lower ($D_{min} = 0.01$) limits, respectively. The blue trajectory shows that $D(t)$ rises quickly to about 0.87 and then stabilizes within the permissible range, demonstrating effective and stable control action.

B. Application under variations

After confirming the stability and performance of the SEPIC converter under constant conditions, it is necessary to evaluate the robustness of the MPC when the system is under operation variations, such as changes in voltage (input or output) and load behavior. To analyze this, three variation scenarios are considered: a four-step change in the output voltage reference, a four-step variation in input voltage and four-step change in load resistance. The tests are shown on Fig. 11, 12 and 13. Fig. 11. Four-step V_o under constant V_{in} and R_{load}. The four-step output voltage is shown in Fig. 11, at t = 1ms it passes from 15V to 24V, at t = 2ms it passes to 48V and at t = 3ms it passes to 60V and sets up. Every transition is quickly reached, and the output voltage follows the references given, even though the variations, which means that the system is stable. Fig. 12. Four-step V_{in} under constant V_o and R_{load}. The four-step input voltage is shown in Fig. 12, with a constant output voltage reference. At first, 20V is introduced as an input voltage. At t = 1ms, it is changed to 30V. At t = 2ms, it is changed to 48V. At t = 3ms, it is changed to 60 and continues. Although the variations of the input voltage, the system keeps following its given reference. Fig. 13. Four-step resistance load under constant V_{in} and V_o. In Fig. 13 shown the four-step resistance load under constant input and output voltage, the system is under a variation of R_{load}=8, 11.5, 15 and 20Ω. In every step of an applied R_{load}, the reference voltage is reached with stability and no overshoot.

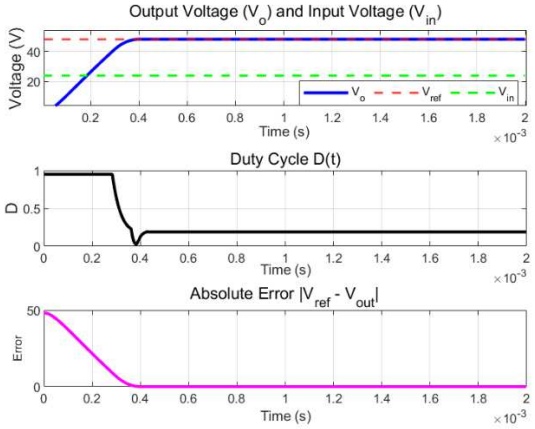


Fig. 8. Output voltage, duty cycle and absolute error in the second application

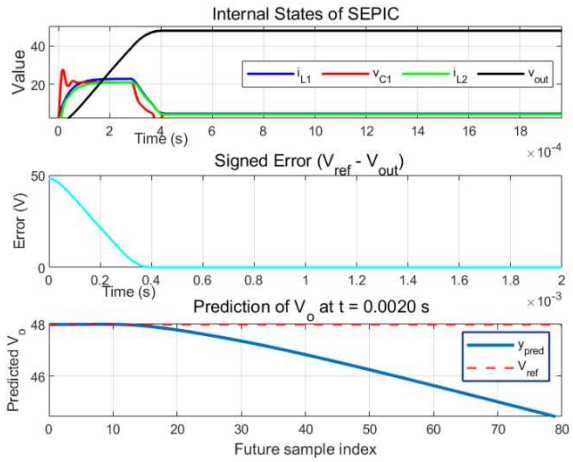


Fig. 9. Internal states of SEPIC signed error and prediction of output voltage in the second application

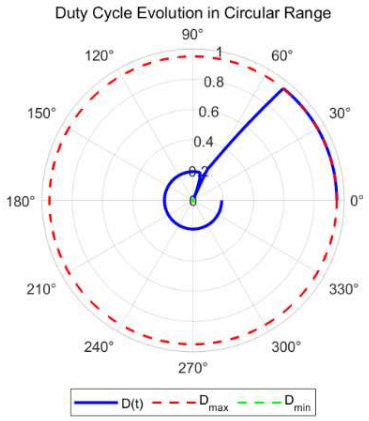


Fig. 10. Duty cycle evolution

Authorized licensed use limited to: ULAKBIM UASL - KARADENIZ TECHNICAL UNIVERSITY. Downloaded on December 31,2025 at 11:57:25 UTC from IEEE Xplore. Restrictions apply.

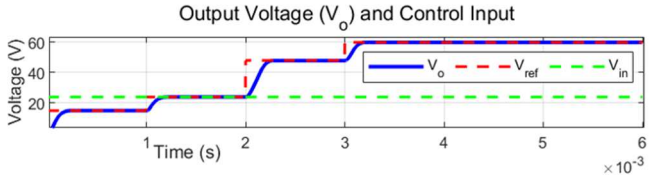


Fig. 11. Four-step V_o under constant V_{in} and R_{load}

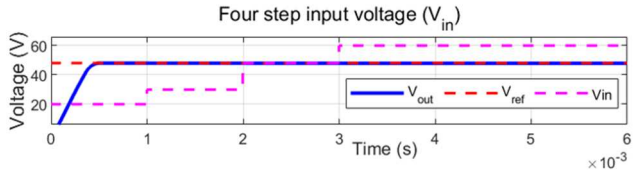


Fig. 12. Four-step V_{in} under constant V_o and R_{load}

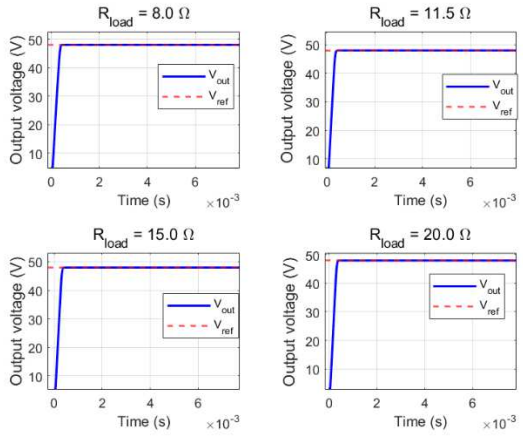


Fig. 13. Four-step resistance load under constant V_{in} and V_o

V. CONCLUSION

This study presented the design and tuning of a Model Predictive Control (MPC) scheme for a Single-Ended Primary-Inductor Converter (SEPIC), emphasizing stability, dynamic performance, and robustness under parameter and load variations. Using a discrete-time state-space model, the controller was first evaluated under nominal conditions and then optimized through an ITAE-based analysis to determine effective weighting parameters Q and R_{mpc}. The optimized configuration significantly improved system stability and transient behavior. Simulation results under varying reference, input, and load conditions demonstrated accurate tracking, minimal overshoot, and rapid settling. These outcomes confirm that the proposed ITAE-driven MPC offers a robust and efficient control solution for SEPIC converters, ensuring reliable operation under diverse real-world scenarios. Future work will focus on implementing the proposed MPC scheme on a real-time digital control platform to experimentally validate its performance under practical operating conditions.

REFERENCES

[1] K. Górecki and K. Detka, "Influence of the Material of Inductor Core on SEPIC Converter Characteristics," in Proceedings - EUROCON 2025: 21st International Conference on Smart Technologies, Institute of Electrical and Electronics Engineers Inc., 2025. doi: 10.1109/EUROCON64445.2025.11073411.

[2] M. Pourmahdi, H. Heydari-Doostabad, N. Zhao, and T. O'Donnell, "Input Admittance Analysis of SEPIC Power Factor Correction Grid-Connected Rectifier," in 2025 IEEE Kiel PowerTech, IEEE, Jun. 2025, pp. 1–7. doi: 10.1109/PowerTech59965.2025.11180318.

[3] G. Vacheva, P. Stanchev, and N. Hinov, "Tolerance Analysis of SEPIC DC-DC Converter," in 2025 19th International Conference on Electrical Machines, Drives and Power Systems, ELMA 2025 - Proceedings, Institute of Electrical and Electronics Engineers Inc., 2025. doi: 10.1109/ELMA65795.2025.11083455.

[4] N. T. Duc, N. H. Viet, P. D. Dai, and B. Van Dai, "Two Stage Single Phase PV System Using SEPIC Converter," in Proceedings of the 2025 17th International Conference on Electronics, Computers and Artificial Intelligence, ECAI 2025, Institute of Electrical and Electronics Engineers Inc., 2025. doi: 10.1109/ECAI65401.2025.11095557.

[5] G. Gökkuş and M. S. Endiz, "Simplified P&O MPPT Algorithm for Accurate Power Tracking in Photovoltaic Systems," Institute of Electrical and Electronics Engineers (IEEE), Sep. 2025, pp. 217–221. doi: 10.1109/iccta65425.2025.11165910.

[6] A. K. Mishra, P. K. Nanda, D. Das, A. K. Patra, N. Nahak, and L. M. Sathapathy, "PID and FOPID Controller Based SEPIC and Cuk Converter for PFC," in 2023 International Conference in Advances in Power, Signal, and Information Technology, APSIT 2023, Institute of Electrical and Electronics Engineers Inc., 2023, pp. 210–214. doi: 10.1109/APSIT58554.2023.10201788.

[7] J. Kathiresan, S. K. Natarajan, and G. Jothimani, "Design and implementation of modified SEPIC high gain DC-DC converter for DC microgrid applications," International Transactions on Electrical Energy Systems, vol. 31, no. 8, Aug. 2021, doi: 10.1002/2050-7038.12921.

[8] M. Fakhry, M. Saber, M. E. Eltantawi, S. S. Kaddah, and B. M. Badr, "DESIGN AND ANALYSIS OF CONTROLLED SEPIC AND LLC CONVERTERS FOR PHOTOVOLTAIC SYSTEMS," 2020. [Online]. Available: http://www.ijeast.com

[9] S. I. Khather and M. A. Ibrahim, "Modeling and simulation of SEPIC controlled converter using PID controller," International Journal of Power Electronics and Drive Systems, vol. 11, no. 2, pp. 833–843, Jun. 2020, doi: 10.11591/ijpeds.v11.i2.pp833-843.

[10] M. O. Ali and A. H. Ahmad, "Design, modelling and simulation of controlled sepic dc-dc converter-based genetic algorithm," International Journal of Power Electronics and Drive Systems, vol. 11, no. 4, pp. 2116–2125, Dec. 2020, doi: 10.11591/ijpeds.v11.i4.pp2116-2125.

[11] S. Mouslim, M. Oubella, M. Kourchi, and M. Ajaamoum, "Simulation and analyses of SEPIC converter using linear PID and fuzzy logic controller," in Materials Today: Proceedings, Elsevier Ltd, 2020, pp. 3199–3208. doi: 10.1016/j.matpr.2020.04.506.

[12] A. L. Jamadar, P. M. Meshram, H. B. Gobburi, and V. B. Borghate, "Modelling and Controller Design of Sepic Converter," in IEEE 1st International Conference on Ambient Intelligence, Knowledge Informatics and Industrial Electronics, AIKIIE 2023, Institute of Electrical and Electronics Engineers Inc., 2023. doi: 10.1109/AIKIIE60097.2023.10390066.

[13] DANAYİYEN Yahya, ALTAŞ İsmail H., and ŞAHİN E, "Model Predıctıve Control of a DC-DC Buck Converter," Sigma Journal of Engineering and Natural Sciences, vol. 8, pp. 91–7, 2017, Accessed: Oct. 22, 2025. [Online]. Available: https://sigma.yildiz.edu.tr/article/511

[14] Y. Danayiyen, K. Lee, M. Choi, and Y. I. Lee, "Model predictive control of uninterruptible power supply with robust disturbance observer," Energies (Basel), vol. 12, no. 15, 2019, doi: 10.3390/en12152871.

[15] O. Abdel-Rahim, M. L. Alghaythi, M. S. Alshammari, and D. S. M. Osheba, "Enhancing Photovoltaic Conversion Efficiency with Model Predictive Control-Based Sensor-Reduced Maximum Power Point Tracking in Modified SEPIC Converters," IEEE Access, vol. 11, pp. 100769–100780, 2023, doi: 10.1109/ACCESS.2023.3315150.

[16] V. Kandasamy, J. Ramprabu, S. Bharaneetharan, P. Abishek, and J. Pradeep, "Enhancement of Electric Vehicle Battery Charging Systems Through the Integration of Interleaved Single-Ended Primary Inductor Converters (SEPIC) and Advanced Model Predictive Control (MPC)," in 2025 International Conference on Advances in Renewable Energy and Electric Vehicles, AREEV 2025, Institute of Electrical and Electronics Engineers Inc., 2025, pp. 89–94. doi: 10.1109/AREEV64307.2025.10925200.

Authorized licensed use limited to: ULAKBIM UASL - KARADENIZ TECHNICAL UNIVERSITY. Downloaded on December 31,2025 at 11:57:25 UTC from IEEE Xplore. Restrictions apply.